Radiography 30 (2024) 359–366

Contents lists available at ScienceDirect

Radiography

journal homepage: www.elsevier.com/locate/radi

Gridless adult cervical spine radiography and its' effect on image quality and radiation dose: A phantom study

N. Mekis [a,*], T. Bianchi [b], C. Doyle [c], M. Gauchat [b], I. Geerling [d], J. Linneman [d], S. Staats [e], C. Campeanu [b]

[a] University of Ljubljana, Medical Imaging and Radiotherapy Department, Zdravstvena Pot 5, 100 Ljubljana, Slovenia
[b] Department of Technical Medical Radiology, School of Health Sciences (HESAV), University of Applied Sciences and Arts of Western Switzerland (HES-SO), Av. de Beaumont 21, 1011 Lausanne, Switzerland
[c] Radiography and Diagnostic Imaging, School of Medicine, University College Dublin, Belfied, Dublin 4, D04 V1W8 Ireland
[d] Department of Medical Imaging and Radiation Therapy, Hanze University of Applied Sciences, Petrus Driessenstraat 3, 9714 CA Groningen, the Netherlands
[e] Radiography in Diagnostics, Department of Clinical Sciences, Central University of the Technology, Bloemfontein, South Africa

A R T I C L E I N F O

Article history:
Received 9 July 2023
Received in revised form
27 November 2023
Accepted 13 December 2023
Available online 22 December 2023

Keywords:
Antero-posterior C-spine
Lateral C-spine
Anti-scatter grid
Digital radiography
Image quality
Dose reduction

A B S T R A C T

Introduction: Imaging of the cervical spine in general radiography is most frequently performed using an anti-scatter grid. The purpose of this study was to investigate the effects of a gridless setting on image quality and radiation dose during digital radiography of the anteroposterior (AP) and lateral (LAT) cervical spine.
Methods: A phantom study was performed with a variety of tube voltages (63–75 kV) with and without an anti-scatter grid. The tube current time product (mAs) and dose area product (DAP) were recorded and used to calculate effective dose (ED) and individual organ dose using PCXMC 2.0 software, as well as entrance surface dose (ESD) and objective image quality: signal-to-noise ratio (SNR) and contrast-to-noise ratio (CNR). Subjective visual image quality grading characteristics (VGC) was performed by five qualified radiographers.
Results: In a gridless setting, the AP and LAT positions showed significantly lower DAP (1.6 μGym^2; 61.3 % and 1.6 μGym^2; 51.2%), ESD (27.6 μGy; 57.3% and 77.2 μGy; 47.2%) and ED (4.2 μSv; 61.3% and 2.3 μSv; 48.9%). In a gridless setting in the AP position, there is a slight significant deterioration in image quality. In the lateral projection, on the other hand, the image quality without the use of grid was only significantly reduced in three of six criteria and there was no difference in the objective image quality between the two settings examined.
Conclusion: The results of this study show that gridless setting significantly decreases radiation dose and image quality, but the quality in the lateral projection is still acceptable for diagnostic purpose.
Implications for practice: The protocol without the use of the anti-scatter grid in cervical spine radiography leads to a reduction in the radiation dose in both projections, but the image quality in the AP is significantly reduced for all criteria examined, with a slight deterioration in image quality in the lateral projection.

Introduction

The responsibility of a radiographer during an X-ray examination is to balance image quality with radiation dose. Image quality should be "as good as necessary, not as good as possible".[1] This stems from the main principle of radiation protection, which states that radiation exposure should be kept As Low As Reasonably Achievable (ALARA). Any step taken to reduce dose is beneficial to the patient if diagnostic image quality is maintained.[2] One of the factors affecting image quality is the scattered radiation reaching the image detector. The amount of scattered radiation depends on the volume of the patient and the tube voltage (kV) (3). The amount of scattered radiation depends on the volume of the patient and the tube voltage (kV).[3] The guidelines recommend the use of anti-scatter grids starting at an anatomic region thickness of 10–12 centimeters (cm).[3,4] According to these recommendations, an anti-scatter grid needs to be used for radiographs of large anatomic volumes, such as the thoracic and lumbar spine. The

* Corresponding author. Zdravstvena pot 5, 1000 Ljubljana, Slovenia.
E-mail address: nejc.mekis@zf.uni-lj.si (N. Mekis).

https://doi.org/10.1016/j.radi.2023.12.009
1078-8174/

practice of using a grid for radiographs of the cervical spine (C-spine) varies among diagnostic imaging departments and among radiographers within the same department.[5] Furthermore, cervical spine radiography is one of the most commonly performed examinations in Europe.[6] It is well known that gridless examinations require a lower radiation dose, the purpose of this study is to investigate whether the absence of an anti-scatter grid can provide images of diagnostic quality during anteroposterior (AP) and lateral (LAT) radiography of the cervical spine. Therefore, a comparison of image quality and radiation dose with and without an anti-scatter grid was performed.

Methods

The complete methodology used in this study is described in detail in the following sections. Ethics committee approval was not obtained because the study was performed on the phantom and not on the patient, and therefore it is not applicable in the country where the study was performed.

Settings

This experimental quantitative study was performed in the Radiography lab at the Faculty of Health Sciences, University of Ljubljana (SLO). All measurements were performed using the Siemens Multix/Vertix unit (Siemens, Germany) with focal spot sizes of 0.6 mm and 1.0 mm, total filtration of 2.5 mm Al (which is in accordance whit our national legislation), and an anti-scatter grid. The grid ratio is 13:1 with 70 lines per cm and an optimal source image distance (SID) of 150 cm. A quality control procedure was performed prior to the measurements. In this test, tube voltage accuracy, reproducibility, half-value layer, current-time product linearity, tube output, total filtration and the dose area-product (DAP) meter accuracy were quality controlled. The results were in accordance with the manufacturers' standards.[7] An amount of 96 images were acquired using AGFA DX -D 40 C (AGFA, Belgium) digital detector.

Phantom

An anthropomorphic phantom PBU-60 simulating a patient with a height of 165 cm and a weight of 50 kg was used. The thickness of the phantoms neck (from C 1 to C6) was 10 cm, and the thickness at the part of the C7/T1 junction was 30 cm. Imaging of the C-spine was performed in the AP (Fig. 1.1) and LAT (Fig. 1.2) positions. The phantom positioning was performed according to the literature.[8] For the AP projection, the phantom was placed supine on the X-ray table with the central beam directed at the thyroid cartilage and the use of cranial angulation of 15°. For lateral projection, the phantom was placed supine on a movable trolley next to the bucky wall stand with the central beam horizontal and the centering point on the thyroid cartilage.

Exposure settings

The AP images have been acquired on the examination table at a SID of 115 cm and with a cranial angulation of 15°, and images in LAT projection were acquired on the Bucky wall stand at a SID of 150 cm to reduce magnification due to the object-detector distance added by the shoulders. The mentioned SID values were the same for gird and gridless setting. For the study, three acquisitions for each kV were taken to limit variance and obtain mean values. Between each exposure, the phantom and X-ray unit were moved and repositioned to incorporate positioning errors into the measurements to simulate a real patient in a clinical setting. The range of kV parameters for the C-spine given in the European guidelines[1] is in the range of 65–75 kV. To reduce the effects of the scattering effect, especially in the gridless setting, two levels below the recommended tube voltage settings were used (63 kV and 64.5 kV). A constant collimation at the detector size of 17 cm × 14 cm for the AP C-spine and 18 cm × 24 cm for the LAT C-spine was used. A small focal spot of 0.6 mm was used for the images of the AP and LAT positions. An automatic exposure control (AEC) mode was selected using the central chamber according to European guidelines.[1] The mAs and DAP values were recorded on the X-ray unit for each exposure. The source phantom distance (SPD) was measured during the experiment. The SPD was 96.0 cm and 119.0 cm for the position AP and LAT, respectively.

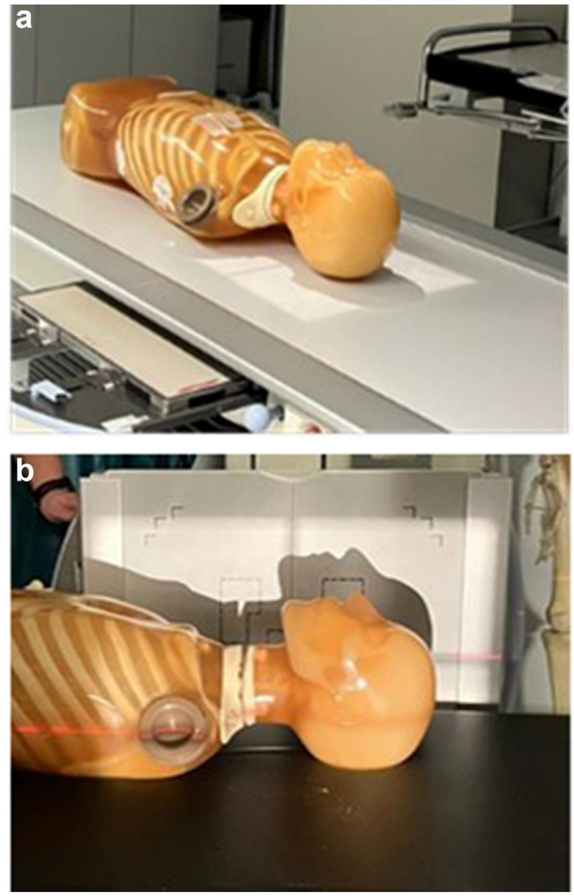

Figure 1. (a) Phantom in AP position. (b) Phantom in LAT position.

Dose calculation

The entrance surface dose (ESD) was calculated from the tube output with the use of equation stated below[9]:

$$ESD = BSF \times Y(d) \times (100/SPD)^2 \times It$$

Where BSF is backscatter factor, Y(d) signifies the tube output per mAs measured at the distance of 100 cm. Source to phantom distance (SPD) was used to calculate the tube current-time product. The BSF has been defined according to the kV, which is 1.31 for 60 kV, 1.32 for 65 kV, 1.33 for 70 kV and 1.34 for 75 kV.[10] Y(d) output was calculated by using measured tube output per mAs for each tube voltage used. The tube output was measured by using a dosimeter (Raysafe ThinX, Sweden), the measurements were done before the experiment started. And the It meaning the tube loading during the exposure (mAs).

Effective dose (ED) and organ dose were calculated using PCXMC 2.0 software (Radiation and Nuclear Safety Authority, Helsinki, Finland). The PCXMC 2.0 software uses the Monte Carlo method to calculate organ dose and effective dose (based on ICRP 103 weighting factors) from patients undergoing radiography. For each exposure, the tube potential, anode angle, beam filtration, and DAP were used to calculate the effective dose and organ dose. The organs with the highest absorbed dose (>2 μGy) are used for this study.

Objective image evaluation

Objective image quality evaluation was performed with the use of ImageJ Fiji software V1.53 (Wayne Rasband and contributors, National Institute of Health, USA). Signal-to-noise ratio (SNR) and contrast-to-noise ratio (CNR) were determined by placing two regions of interest (ROI's) inside and outside the phantom anatomy. Measurements were performed on a total of 96 images. The CNR and SNR were calculated using the following formulas[11]:

CNR = 20 log10((m1-m2)/std2)
SNR = 20 log10(m/std2)
m1 – average ROI1
m2 – average ROI2 (background)
m – average value from the complete image
std2 – standard deviation from ROI2.

The measurements on the AP and LAT images were performed on the part of the image with the highest attenuation and on the part of the lowest attenuation as shown on Figs. 2 and 3.

Subjective image evaluation

Subjective image assessment was performed using visual grading characteristics (VGC) using ViewDEX 2.57 software.[12,13] According to the recommendations of the European Commission,[1] the criteria for an optimal image that applies to the AP and LAT projection of the C- spine are described in Table 1. For both images, an additional criterion 'overall image quality' was added. The evaluator were allowed to change the window of the image based on their preferences.

Images from each exposure setting (kV) were randomly selected (n = 32). The evaluators (five radiographers with a minimum experience of 4 years) were asked to evaluate these 32 images (16 in the AP projection and 16 in the LAT projection). The image evaluation was blinded so that the evaluator did not know the exposure parameters in which the images were taken. Besides that, the image representation was randomized so the order of the representation of the images for each evaluator was unique. The

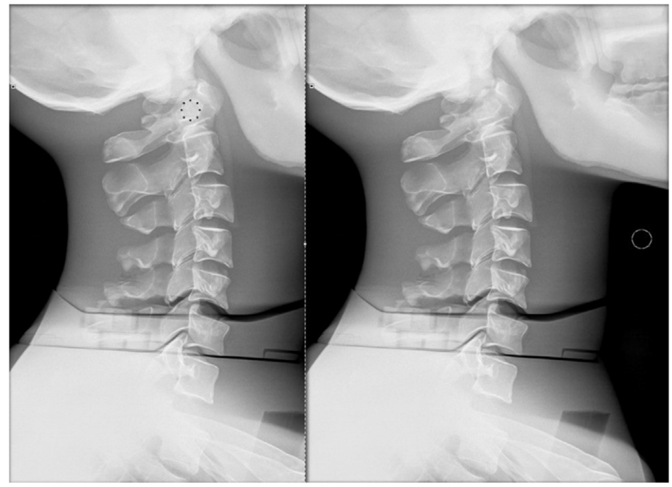

Figure 3. The region-of interest on the part of the image with the highest attenuation and for the part of the lowest attenuation on the LAT projection.

Table 1
Criteria for an optimal image that applies to the AP and LAT projection of the C-spine.

Criteria AP	
1	Complete imaging of the cervical spine, including the upper cervical spine and the 7th vertebra
2	Visually sharp imaging, as a single line, of the upper and lower-plate surface in the centred beam area
3	Visualization of the intervertebral joints and the spinous processes
4	Visually sharp imaging of the cortical and trabecular structures
5	Overall image quality
Criteria LAT	
1	Complete imaging of the cervical spine, including the upper cervical spine and the 7th vertebra
2	Visually sharp imaging, as a single line, of the upper and lower-plate surface in the centred beam area
3	Visualisation of the intervertebral spaces, intervertebral joints and spinous processes
4	Visualisation of the soft tissues, particularly the retro tracheal space
5	Visually sharp imaging of the cortical and trabecular structures
6	Overall image quality

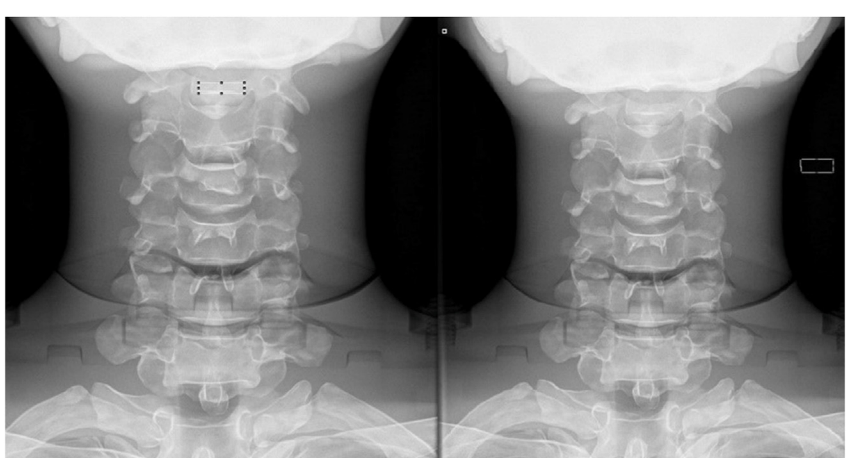

Figure 2. The region-of interest on the part of the image with the highest attenuation and for the part of the lowest attenuation on the AP projection.

images were evaluated on a Barco MDCG 3120 diagnostic monitors, with active screen diagonal 582 mm, resolution 3 MP, pixel pitch 0.2070 mm and 1024 grey levels (Barco, Belgium). The room lightning condition was 10 lux (measured with RaySafe X2 light sensor, Sweden), and the evaluators sat directly in front of the screen at arm's length distance. Scoring was based on a four-point scale, with “1” a diagnostically inadequate image, “2” a moderate diagnostic image, “3” a good diagnostic image, and “4” perfect diagnostic image. The results were then extracted from the software and an average from all five evaluators was calculated for each criterion as well as the sum of all averages represented a total score, which was then compared (with and without the use of the anti-scatter grid).

Statistic tests

The software IBM SPSS 26.0 (IBM, USA) was used to analyze the results with the Shapiro–Wilk test to determine the normal distribution of the sample and the reliability of the radiographers. If the data were normally distributed, an independent samples T-test was used to compare the differences between the use of a grid vs no grid. If the data were not normally distributed, a Mann Whitney U test was used. ICC values were used to determine the reliability of the evaluators. ICC values less than 0.5 indicate poor reliability, values between 0.5 and 0.75 indicate moderate reliability, values between 0.75 and 0.9 indicate good reliability, and values above 0.90 indicate excellent reliability.[14,15] The significance level of $p < 0.05$ was used for all tests.

Results

A total of 96 images were acquired for AP (n = 24 without gird; n = 24 with grid) and LAT projection (n = 24 without gird; n = 24 with grid) of the C-spine. The PCXMC 2.0 software results show that the following organs had the highest absorbed dose values (>2 μGy): extrathoracic airway, lymph nodes, oral mucosa, salivary glands, and thyroid gland. Therefore, these organs were included in this study.

AP projection of the C-spine

The mean difference of DAP value between protocols with use of a grid was 61.3% higher than without use of a grid. The DAP is higher when a grid is used (2.6 μGy m^2) than when a grid is not used (1.0 μGy m^2). In the case of ESD, the mean difference between the two protocols was 57.3% and the mean difference of ED was 61.3%. Table 2 shows the descriptive statistics for DAP, ESD, the effective dose, and the dose to selected organs. While Fig. 4 shows the DAP differences between grid settings across the range of tube voltage settings.

The mean difference between images without and with grid was calculated for all criteria evaluated: “Complete imaging of the cervical spine, including the upper cervical spine and the 7th vertebra” (13%), “Visually sharp imaging of the upper and lower plate surface in the centered beam area” (21.3%), “Visualisation of the intervertebral joints and spinous processes” (24.9%), “Visually sharp imaging of the cortical and trabecular structures” (20.8%), ‘Overall image quality’ (20.8%), and Total IQ (20.5%) in favour of the protocol using the grid. For the objective measurements of the IQ, the results were similar to the VGC analysis with a smaller difference between the grid and gridless protocols; CNR (7.0%) and SNR (7.6%). The descriptive statistic values of all the IQ assessment are shown in Table 3. While Fig. 5 shows the DAP differences between grid settings across the range of tube voltage settings.

Table 4 represents the ICC scores for each separate criterion for all the 5 evaluators for AP projection of the C-spine.

LAT projection of the C-spine

In the case of the LAT projection the mean difference between the protocol with the use of a grid compared to the gridless protocol was 51.2% for the DAP, 47.2% for the ESD, and 48.9% for the ED. Table 5 presents the descriptive statistics for the DAP, ESD, effective dose, and dose to selected organs in the LAT projection. While Fig. 5 shows the DAP differences between grid settings across the range of tube voltage settings.

Fig. 5 represents the results for the DAP values for each tube voltage and separate for the grid and gridless setting in LAT projection of C-spine.

The mean difference was calculated for images with and without the grid for all the assessed criteria: “Complete imaging of the cervical spine, including the upper cervical spine and the 7th vertebra” (10.8%), “Visually sharp imaging, as a single line, of the upper and lower-plate surface in the centred beam area” (4.7%), “Visualisation of the intervertebral spaces, intervertebral joints and spinous processes” (7.9%), “Visualisation of the soft tissues, particularly the retrotracheal space” (5.4%), “Visually sharp imaging of the cortical and trabecular structures” (9.9%), “Overall image quality” (7.1%), and Total image quality (14.3%) in favour of the protocol using the grid. On the other hand, there were no

Table 2
Descriptive statistics comparison between the two grid settings in C-spine in the AP projection (n = 96).

Variable	Grid	Mean	Median	Std. Deviation	Minimum	Maximum	P-value
DAP (μGy m-2)	no	1.0	1.0	0.1	0.9	1.2	p < 0.001[a]
	yes	2.6	2.6	0.4	2.1	3.2	
ESD (μGy)	no	81.7	80.0	8.8	72.0	94.9	p < 0.001[a]
	yes	191.3	188.5	24.7	161.4	226.5	
Effective dose (μSv)	no	2.6	2.5	0.3	2.3	3.0	p < 0.001[a]
	yes	6.8	6.8	0.8	5.7	7.8	
Extrathoracic airways (μGy)	no	21.3	20.8	2.1	19.1	24.3	p < 0.001[a]
	yes	55.9	56.0	6.5	47.2	63.8	
Lymph nodes (μGy)	no	6.5	6.4	0.6	5.8	7.5	p < 0.001[a]
	yes	17.2	17.2	2.0	14.4	19.6	
Oral mucosa (μGy)	no	6.7	6.6	0.5	6.2	7.5	p < 0.001[a]
	yes	17.7	17.7	1.6	15.6	19.6	
Salivary glands (μGy)	no	16.6	16.2	1.4	15.0	18.7	p < 0.001[a]
	yes	43.5	43.6	4.6	37.2	49.2	
Thyroid (μGy)	no	46.3	45.1	5.0	41.0	53.4	p < 0.001[a]
	yes	121.6	121.6	15.6	100.6	140.2	

[a] T-test for independent samples; estimated PCXMC errors are 0.3% for ED, 0.4% for extrathoracic airways, 0.2% for lymph nodes, 0.6% for oral mucosa, 0.4% for salivary glands and 0.4% for thyroid.

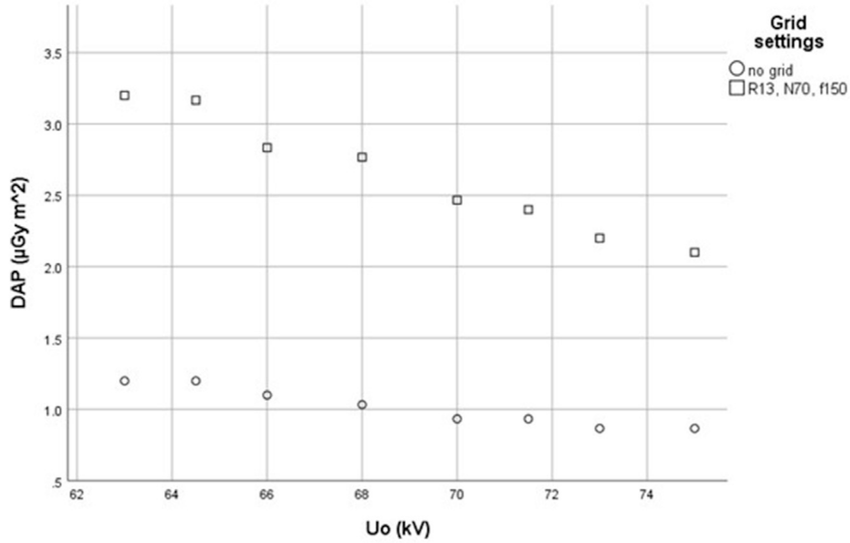

Figure 4. Results for DAP based on the tube voltage used and the use of grid settings.

Table 3
Descriptive statistical comparison between grid vs no grid for VGC scores in the AP projection (n = 32) (subjective evaluation), CNR and SNR (objective evaluation) (n = 96).

Variable	Grid	Mean	Median	Std. Deviation	Minimum	Maximum	p - value
Criterion 1	no	2.0	1.9	0.2	1.8	2.4	p = 0.028[a]
	yes	2.3	2.3	0.2	2.0	2.6	
Criterion 2	no	2.6	2.6	0.2	2.4	2.8	p < 0.001[b]
	yes	3.3	3.2	0.2	3.0	3.6	
Criterion 3	no	2.4	2.3	0.3	2.0	2.8	p < 0.001[a]
	yes	3.1	3.1	0.2	3.0	3.4	
Criterion 4	no	2.4	2.4	0.3	2.0	2.8	p < 0.001[b]
	yes	3.0	3.0	0.2	2.8	3.2	
Criterion 5	no	2.4	2.4	0.2	2.0	2.6	p = 0.005[a]
	yes	3.0	3.0	0.2	2.8	3.4	
Total IQ	no	11.7	11.8	0.8	10.6	12.8	p < 0.001[b]
	yes	14.8	14.7	0.6	14.0	15.8	
CNR (dB)	no	46.6	45.8	2.2	45.0	51.4	p = 0.005[a]
	yes	50.1	49.4	1.8	48.4	53.4	
SNR (dB)	no	42.8	41.9	2.2	41.2	47.6	p = 0.005[a]
	yes	46.4	45.6	1.8	44.6	49.6	

[a] Mann Whitney U test.
[b] Independent samples T-test.

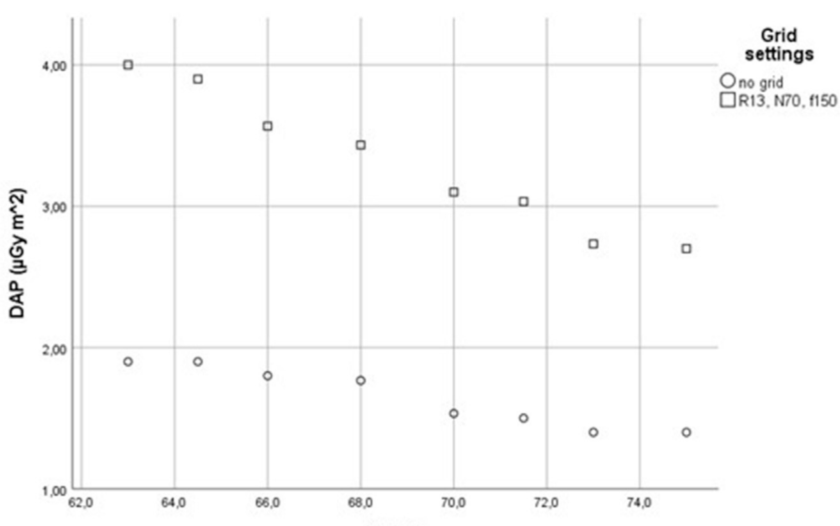

Figure 5. Scatter plot representation of the results for DAP based on the tube voltage used and the use of grid settings for the LAT position.

Table 4
ICC results for the AP projection of C-spine.

Variable	Intraclass Correlation Coefficient	Reliability
Criterion 1	0.470	Poor reliability
Criterion 2	0.783	Good reliability
Criterion 3	0.803	Good reliability
Criterion 4	0.726	Good reliability
Criterion 5	0.793	Good reliability

statistically significant differences in objective OQ measures (CNR (−0.6%) and SNR (−0.5%)). The entire set of the descriptive statistics is shown in Table 6.

Table 7 represents the ICC scores for each separate criterion for all the 5 evaluators for the images in the LAT projection of the C-spine.

Table 7
ICC results for the LAT projection of C-spine.

Variable	Intraclass Correlation Coefficient	Reliability
Criterion 1	0.324	Poor reliability
Criterion 2	−0.424	Poor reliability
Criterion 3	0.383	Poor reliability
Criterion 4	0.418	Poor reliability
Criterion 5	0.307	Poor reliability
Criterion 6	0.372	Poor reliability

Discussion

The aim of this study was to investigate whether the absence of an anti-scatter grid can provide images of diagnostic quality in accordance with the ALARA principle. In this study an expected reduction in dose was observed for the AP and LAT projections when removing the grid across DAP, ESD, and ED. Without the use of the anti-scatter grid resulted in a reduction of 61.5% (DAP), 57.3% (ESD), and 61.9% (ED), respectively, for the AP projection of the cervical spine. However, the differences in absolute values were low if we look from the point of clinical significance. The reduced dose correlates with the study by Roberts et al.,[16] who also found a reduced ED in the absence of a grid. The results of Moey et al.[5] stated that a higher kV value corresponded with a lower mAs value and thus a lower ESD. In our study all images, with a higher kV value corresponded to a lower mAs value when AEC was used.

Table 5
Descriptive statistic comparison between the use of two grid settings in C-spine in lateral projection (n = 96) for C-spine in LAT projection.

Variable	Grid	Mean	Median	Std. Deviation	Minimum	Maximum	p - value
DAP (μGy mˆ2)	no	1.7	1.7	0.2	1.4	1.9	p < 0.001[b]
	yes	3.3	3.3	0.5	2.7	4.0	
ESD (μGy)	no	86.5	85.2	10.0	74.7	100.9	p < 0.001[b]
	yes	163.7	161.3	20.6	139.1	192.6	
Effective dose (μSv)	no	2.4	2.4	0.2	2.2	2.6	p < 0.001[b]
	yes	4.7	4.7	0.7	3.5	5.4	
Extrathoracic airways (μGy)	no	17.9	18.0	1.4	16.2	19.6	p < 0.001[b]
	yes	35.3	35.6	4.5	26.8	40.3	
Lymph nodes (μGy)	no	5.7	5.7	0.5	5.1	6.2	p < 0.001[b]
	yes	11.2	11.2	1.4	8.9	12.8	
Oral mucosa (μGy)	no	8.3	8.4	0.6	7.6	9.0	p < 0.001[a]
	yes	18.0	17.2	3.3	15.2	25.7	
Salivary glands (μGy)	no	15.8	15.9	1.4	14.2	17.4	p < 0.001[b]
	yes	32.7	32.9	3.1	27.9	35.9	
Thyroid (μGy)	no	37.6	37.7	3.5	33.3	41.7	p < 0.001[b]
	yes	72.6	74.4	13.4	44.4	85.8	

[a] Mann Whitney U-test.
[b] T-test for independent samples; estimated PCXMC errors are 0.3% for ED, 0.7% for extrathoracic airways, 0.4% for lymph nodes, 0.6% for oral mucosa, 0.4% for salivary glands and 0.5% for thyroid.

Table 6
Descriptive statistical comparison between grid vs no grid for VGC scores in LAT projections (n = 32) (subjective evaluation), CNR and SNR (objective evaluation) (n = 96) for C-spine lateral projection.

Variable	Grid settings	Mean	Median	Std. Deviation	Minimum	Maximum	p - value
Criterion 1	no	2.5	2.5	0.2	2.2	2.6	p = 0.007[b]
	yes	2.8	2.8	0.2	2.4	3.0	
Criterion 2	no	3.0	3.0	0.1	2.8	3.2	p = 0.234[b]
	yes	3.2	3.1	0.2	3.0	3.6	
Criterion 3	no	2.3	2.4	0.2	2.0	2.6	p = 0.161[b]
	yes	2.5	2.6	0.3	2.0	3.0	
Criterion 4	no	2.6	2.6	0.2	2.2	2.8	p = 0.195[b]
	yes	2.8	2.9	0.4	2.0	3.2	
Criterion 5	no	2.8	2.8	0.3	2.4	3.2	p = 0.382[b]
	yes	3.0	2.9	0.2	2.8	3.4	
Criterion 6	no	2.7	2.7	0.2	2.6	3.0	p = 0.021[b]
	yes	3.0	3.0	0.3	2.4	3.4	
Total IQ	no	16.0	16.3	0.8	14.2	16.8	p = 0.021[b]
	yes	17.2	17.3	1.4	14.8	19.6	
CNR (dB)	no	46.0	45.8	0.5	45.4	46.8	p = 0.220[a]
	yes	45.7	45.7	0.2	45.3	46.3	
SNR (dB)	no	42.7	42.6	0.4	42.1	43.4	p = 0.306[a]
	yes	42.5	42.5	0.2	42.2	43.1	

[a] Independent samples T-test.
[b] Mann Whitney U test.

All subjective image criteria result that the images obtained in the AP projection were significantly better when a grid was used. The total subjective image quality of the AP images with grid increased by 20.5% compared to those without a grid. The SNR and CNR also showed a statistically significant increase by using the grid of 7.0% for the CNR and 7.61% for the SNR. However, the DAP increased by 61.4% when a grid was present. Use of the grid increases dose more than it decreases the image quality and requires increased mAs and thus increased DAP.

A significant dose reduction was also observed with lateral projection of the C-spine; dose values were reduced by 50.2% (DAP), 47.2% (ESD), and 48.9% (ED). The differences in absolute values was again very low but nevertheless higher than in AP projection. The results of a study by Moey et al. 5 show a 61.1% reduction in ESD when no grid is used in CR radiography. This is consistent with the results of our study. Images from AP projection with and without the use of anti-scatter grid showed a steady decrease in ESD as kV increased. There was no linear decrease of the ESD in the images obtained in the lateral projection. The objective image quality of the LAT C-spine images was not significant. As for the subjective evaluation, the results of the VGC analysis only showed that criteria 1 and 6 were statistically significant for the LAT position: ‘Complete imaging of the cervical spine, including the upper cervical spine and the 7th vertebra’ and ‘Overall image quality’ as well as total image quality. The differences in the values of the other four criteria were not significant, but the image quality was acceptable. Therefore, the lowest DAP will be preferred for LAT images. The airgap effect present in the LAT images decreases the scattered radiation received by the detector, which improves the image quality.[17] Due to the airgap effect in the lateral projection, there is a difference in significance between the results of the AP and LAT projections. With regard to the lateral cervical spine view, it must also be noted that it was not possible to evaluate the differences in larger patient sizes and in patients with large shoulders that cannot be displaced downwards due to the limitations of the phantom shoulders and anatomy.

Earlier research has a clear difference on image quality when a grid is used or not used.[16,18] The research by Moey et al. (5) shows that the use of a grid enhances the image contrast by removing scatter from the image.

The mean values of the IQ criterion for AP and LAT projections are all above the assessment threshold of 2 “moderate” and are therefore clinically acceptable according to the evaluators' assessments. The SNR and CNR also show a statistically significant increase with the use of the grid of 7.0% for CNR and 8.8% for SNR, but only in the case of the AP projection of the C-spine. However, on average for both projections, DAP increased by 61.4% with the use of the grid. The use of the grid increases the dose more than the image quality. The reliability of the first criterion from the subjective evaluation: ‘Complete imaging of the cervical spine, including the upper cervical spine and the 7th vertebra’ was not reliable for the AP images.

As with any study, there were some limitations to our study. The first limitation is that the study was conducted on an anthropomorphic phantom with only one thickness size, so we could not evaluate the effect of thickness change on image quality. The other phantom limitation is that the shoulders don't have the tissue around the joints and therefore the attenuation of the photons is lower than in real patient.

No test images were offered before the start of the VGC. VGC assessment was performed only by 5 professional radiographers and no other professionals like for example radiologists. Two of the five evaluators were very strict due to the lack of adaptation of the criteria, which resulted in the average being affected by these non-standard values and therefore the reliability of the LAT images is low. This corresponds with the ICC values.

According to the criteria for LAT VGC, the soft tissues should be evaluated.[1] However, the antrophomorpic phantom used did not contain a trachea or other air containing structures or landmarks such as a hyoid bone, so the criteria should have been adapted.

Conclusion

This study investigated the effect of a gridless protocol on radiation dose and image quality in cervical spine radiography in AP and lateral projection. The study was performed on an anthropomorphic phantom. It was found that the gridless protocol resulted in a significant reduction in DAP (61.3% and 51.2%), ESD (57.3% and 47.2%) and ED (61.3% and 48.9%) for cervical spine radiographs in AP and lateral projection compared to the grid protocol, as expected based on the literature. In AP projection, a significant deterioration in image quality was observed in both subjective and objective IQ assessment. For lateral projection, there was no significant deterioration in IQ when using the gridless protocol for half of the subjective IQ scores and both objective IQ scores. Based on our results, we can conclude that AP projection should be performed with the use of a grid due to the significant reduction in all IQ criteria studied and the small differences in absolute values of dose reduction. For lateral projection, a significant difference was found in half of the subjective IQ, but there was no difference in objective image quality. It should also be noted that the differences in the absolute dose values examined were higher when comparing the above settings. Based on all the results presented in the phantom study, we as authors suggest that further research is needed to determine the optimal grid settings for cervical spine radiography, especially the results of the patient study with different body habitus.

Conflict of interest statement

N. Mekis holds a Radiography journal international advisory board role. Other authors have no conflict of interest and nothing to declare.

Acknowledgements

This research did not receive any specific grant from funding agencies in the public, commercial, or not-for-profit sectors.

References

1. Busch HP. *Image quality and dose mangement for digital radiography*. 2004.
2. The 2007 recommendations of the international commission on radiological protection. ICRP publication 103. *Ann ICRP* 2007;**37**(2–4):1–332. https://doi.org/10.1016/j.icrp.2007.10.003.
3. Bontrager KL, Lampignano JP. *Textbook of positioning and related anatomy*. 2014.
4. College A. *ACR – AAPM – SIIM – SPR practice parameter for digital*. 2017. p. 1076. Revised 2008).
5. Moey SF, Ramlee NNM. Image quality and entrance surface dose evaluation of lateral cervical spine: a study using grid and non-grid techniques. *Iranian Journal of Medical Physics* 2019;**16**(2):166–70. https://doi.org/10.22038/ijmp.2018.33059.1400.
6. European Union. *Diagnostic Reference Levels in Thirty-six European Countries. Part 1/2*. 2015.
7. Hiles PA, Mackenzie A, Scally A, Wall B. *Recommended standards for the routine performance testing of diagnostic X-ray imaging systems; Repot 91*. York: Institute of Physics and Engineering in Medicine; 2005.
8. Long BW, Rollins JH, Smith BJ, Frank ED. *Merrill's atlas of radiographic positioning & procedures*. 14th ed. St. Louis: Elsevier; 2019.
9. International Atomic Energy Agency. *Dosimetry in diagnostic radiology: an international code of practice*. Vienna: International Atomic Energy Agency; 2007.
10. European Commission. *European guidance on estimating population doses from medical X-ray procedures*. 2008.

11. Desai N, Singh A, Valentino DJ. Practical evaluation of image quality in computed radiographic (CR) imaging systems. Medical Imaging 2010. *Physics of Medical Imaging* 2010:7622. https://doi.org/10.1117/12.844640. May 2014): 76224Q.
12. Börjesson S, Håkansson M, Båth M, Kheddache S, Svensson S, Tingberg A, et al. A software tool for increased efficiency in observer performance studies in radiology. *Radiat Protect Dosim* 2005;**114**(1–3):45–52. https://doi.org/10.1093/rpd/nch550.
13. Ba M. *VIEWDEX: Status Rep* 2016;**169**(1):38–45.
14. Koo TK, Li MY. A guideline of selecting and reporting intraclass correlation coefficients for reliability research. *Journal of Chiropractic Medicine* 2016;**15**(2): 155–63. https://doi.org/10.1016/j.jcm.2016.02.012.
15. Jampol LEEM, Tanna AP, Portney G, Watkins MP, Saddle U, Hall P. *Multimedia Reviews Foundations of Clinical Research: Application* 2002;**47**(6):6257.
16. Roberts JA, Evans SC, Rees M. Optimisation of imaging technique used in direct digital radiography. *J Radiol Prot* 2006;**26**(3):287–99. https://doi.org/10.1088/0952-4746/26/3/003.
17. Bellizzi A, Zarb F. Optimisation of the lateral lumbar spine projection using an air-gap technique. *Radiography* 2020;**26**(3):227–33. https://doi.org/10.1016/j.radi.2019.12.008.
18. Keating M, Grange S. Image quality in the anteroposterior cervical spine radiograph: comparison between moving, stationary and non-grid techniques in a lamb neck. *Radiography* 2011;**17**(2):139–44. https://doi.org/10.1016/j.radi.2010.12.007.